Gelation of fish gelatin studied by multi-particle tracking method

Maki, Yasuyuki
Department of Chemistry, Faculty of Science, Kyushu University

Annaka, Masahiko
Department of Chemistry, Faculty of Science, Kyushu University

出版情報：Food Hydrocolloids. 101, pp.105525-, 2020-04. Elsevier
バージョン：
権利関係：

Gelation of Fish Gelatin Studied by Multi-Particle Tracking Method

Yasuyuki Maki,* Masahiko Annaka

Department of Chemistry, Faculty of Science, Kyushu Universiy, Fukuoka 819-0395, Japan

* Corresponding author. Tel: +81-92-802-4120;

e-mail: maki@chem.kyushu-univ.jp

Abstract

Gelatin from various sources are extensively used as food hydrocolloids. Recently, fish gelatin has attracted special attention because of religious or medical reasons. Most food gels show structural inhomogeneity that may affect their texture and flavor release, although gelatin gels appear transparent and homogeneous. In this study, the local dynamics at the micron scale of the fish gelatin were investigated by using a multiple particle tracking method. The slow gelation of the fish gelatin compared to mammalian gelatin enabled us to study the gelation process in detail. The dynamics of microspheres embedded in the gelatin revealed the transition of gelatin from a homogeneous fluid to an elastic gel that is rheologically inhomogeneous at the micron scale.

Keywords gelatin / gel / inhomogeneity / particle tracking / microrheology

1. Introduction

Gelatin is one of the major food hydrocolloids, and also finds widespread applications in cosmetics, pharmaceutics, and biomedical materials. Gelatin is produced by denaturation and partial hydrolysis of animal tissue collagen (Djabourov, Leblond & Papon, 1998). Although skin and bone of mammals (e.g. porcine, bovine) have been traditionally used as raw materials for gelatin, they are not accepted in some cases because of religious prohibition and a potential risk of zoonoses. Recently, skin or scales of fish attracts attention as an alternative source of gelatin due to religious needs and a low zoonotic risk (Karim & Bhat, 2009; Lin, Regenstein, Lv, Lu & Jiang, 2017).

In decreasing temperature of a dilute solution of gelatin below the transition temperature T_c, gelatin molecules undergo a transition from the random-coil conformation to a partially ordered structure originating from the collagen triple-helix. At concentrations higher than several percent, aqueous gelatin is a fluid at temperatures above T_c, whereas it forms a gel at a temperature below T_c because gelatin molecules partially assume the collagen-like ordered structure, which consists of junction zones of the gel network (Djabourov et al., 1998).

One of the main characteristic of gelatin gel is high transparency. This contrasts with most food gels, which are more or less turbid. Agarose, the main component of agar, forms slightly turbid gel because of phase separation. A recent small-angle light-scattering study revealed that quenched agarose solutions showed spinodal decomposition after the gel network formation (Morita, Narita, Mukai, Yanagisawa & Tokita, 2013). On the other hand, gelatin gels appear transparent because of its relatively homogeneous network structure (Ross-Murphy, 1992), as shown from light scattering and small-angle neutron scattering experiments (Bode, da Silva, Smith, Lorenz, McCullen, Stevens & Dreiss, 2013; Pezron, Herning, Djabourov & Leblond, 1990, Yang, Hemar, Hilliou, Gilbert, McGillivray, Williams & Chaieb, 2015). However, a detailed analysis of scattered light from gelatin in the gelation process showed that a speckle pattern, i.e., a strong intensity variation with sample position, emerged after the gelation (Okamoto, Norisuye & Shibayama, 2001). The speckle pattern was due to frozen inhomogeneity at the micron scale, and was also observed for chemically-crosslinked hydrogels such as *N*-isopropylacrylamide (NIPA) gels (Shibayama, 1998). This indicates that some spatial inhomogeneity could be found even in a transparent gelatin gel. In general, the inhomogeneity of the network structure affects gel properties such as an elastic modulus and transport coefficients, which would be closely correlated with the texture and flavor release of food gels (Weel, Boelrijk, Alting, van Mil, Burger, Gruppen, Voragen & Smit, 2002; Yang, Wang, Brenner, Kikuzaki, Fang & Nishinari, 2015).

In the case that materials have structural inhomogeneity at the micron scale, their rheological properties should be spatially inhomogeneous at the same scale. A multi-particle tracking is a method for probing local dynamics of complex fluids on the scale of microns (microrheology) by analyzing Brownian motion of many microparticles embedded in the samples (Furst & Squires, 2017). In this method, the motion of many particles is recorded

simultaneously while retaining information of the individual trajectory of each particle. Thus, the measurements on ensembles of particles provide statistical accuracy, while spatial heterogeneities can also be revealed. Lately, the multi-particle tracking method has been used to investigate the dynamics of food emulsions and gels because these systems are typically complex and heterogeneous, and the microstructure, local dynamics, and their relation to the macroscopic properties and stability of such systems have attracted much attention (Lu & Corvalan, 2016; Moschakis 2013).

There are a few studies that explored rheological properties of gelatin by the particle tracking method. Shabaniverski et al. used the particle tracking method for measuring viscoelasticity of gelatin solutions of the concentration ranging from 0.3 and 0.6 wt% (Shabaniverski & Juárez, 2017). Hong et al. investigated the time-dependent sol-gel transition of a 6 wt% gelatin solution by the multi-particle tracking method and examined heterogeneity in local dynamics during the gelation process (Hong, Xu, Ou, Sun, Wang & Tong, 2018). In these studies, the particle-tracking experiments were performed for the gelatin solutions of relatively low concentrations, probably because of the immediate formation of highly viscoelastic gels at the higher concentrations. This limitation is attributable to the fact that the particle tracking method is only applicable to soft materials with low rigidity (typically ~ 10^1 Pa) (Breedveld & Pine, 2003) which assures a particle displacement sufficiently larger than the detection resolution under the small driving-forces available from Brownian motion. In the latter study (Hong et al., 2018), the time-resolved measurements were performed at time intervals of 5 min owing to the relatively fast gelation process and thus each measuring period was less than 1 min. For higher gelatin concentrations, the gelation process becomes faster and the measuring times need to be shorter, which may result in a loss of statistical accuracy.

The gel network of gelatin is gradually formed after the quench below the gelling temperature and then slowly matured for very long periods (Normand, Muller, Ravey & Parker, 2000; Ronsin, Caroli & Baumberger, 2009; Te Nijenhuis, 1981a). The rate of the gelation process depends on temperature and the gelatin concentration. At a given concentration, the gelation rate is dominated by the quench depth from the critical gelation temperature, since the quench depth determines the difference in the chemical potential, i.e., the driving force for the gelation process (Ronsin, Caroli & Baumberger, 2017). The critical

gelation temperature of gelatin depends on its raw material. Because of their lower hydroxyproline contents, fish gelatins show a lower critical gelation temperature than mammalian gelatins (Karim & Bhat, 2009). Therefore, if the temperature and the concentration are the same, fish gelatins should undergo slower gelation than mammalian gelatins because of the smaller quench depth. The slower gelation of fish gelatin than mammalian gelatin has been shown in the literature (Yoshimura, Terashima, Hozan, Ebato, Nomura, Ishii & Shirai, 2000). When fish gelatin is used for the particle tracking measurements, instead of mammalian gelatin as in the previous studies (Hong et al., 2018; Shabaniverski et al., 2017), the gelling occurs slowly even at higher concentrations, which enables us to study the gelation process more precisely. Thus, in this study, the gelation of fish gelatin at concentrations ranging from 7.5 to 15 wt% was investigated by the multi-particle tracking method.

2. Materials and methods

Fish gelatin (Type A, Bloom 250) was kindly donated by Nitta Gelatin Inc., Japan. The gelatin was mainly extracted from the skin of tilapia and golden threadfin bream, according to the supplier. The pH of the gelatin solution was 5.9. The gelatin was dissolved in deionized water at 50 ^{o}C and then polystyrene microspheres of 600 nm diameter (Thermo Fisher Scientific Inc., Fremont, CA) were added as probe particles. The solution was prepared at four gelatin concentrations ranging from 7.5 to 15 wt% and the concentration of the probe particles was approximately 0.0006 %. Because of the low concentration of the particles, the effect of the presence of the particles on the rheological properties of the sample is negligible. The solutions and gels of the fish gelatin were as transparent as those of porcine skin gelatin (Type A, Bloom 250) from Nitta Gelatin Inc., Japan (Supplementary material, S1). The critical gelation temperature of the fish gelatin depended on the concentration and ranged from 27 ^{o}C (7.5 wt%) to 30 ^{o}C (15 wt%) (Supplementary material, S2). The values of G' and G'' for 10 wt% gelatin measured at 330 min after the quench to 25 ^{o}C were 69 Pa and 18 Pa, respectively (Supplementary material, S3). The solution was injected to a chamber consisting of a coverslip and microscope slide, and the chamber was sealed with nail polish. The sample chamber warmed on a heater at 40 ^{o}C was quench cooled to 25 ^{o}C by transferring the chamber

to a stage of an inverted microscope equipped with a CMOS camera and then videos were recorded at appropriate time intervals after the quench. The size of the field of view was 117.7 μm × 93.2 μm and the video frame rate was 24 fps. The displacement of the probe particles was measured by analyzing the video images using ImageJ software (NIH) and a particle track and analysis plugin for ImageJ (https://github.com/arayoshipta/projectPTAj). In order to quantify the dynamics of the probe particle motion reflecting the rheological properties of gelatin, the mean square displacement (MSD) was calculated with the following equation,

$$\langle \Delta r^2(\tau) \rangle = \frac{1}{N} \sum_i \langle |\mathbf{r}_i(t+\tau) - \mathbf{r}_i(t)|^2 \rangle, \qquad (1)$$

where $\mathbf{r}_i$ (= (x_i, y_i)) is centroid position of the ith particle in the two dimensions, N is the number of the probe particles, τ is the lag time, and $\langle \quad \rangle$ represents the time average. The MSD for the particles immobilized on the glass surface was measured and used for the correction of the static error (Savin & Doyle, 2005). In addition, we calculated the probability density function (PDF) of particle displacements, or the van Hove correlation function, defined as

$$P(x,\tau) = \sum_i \langle \delta(x - [x_i(t+\tau) - x_i(t)]) \rangle, \qquad (2)$$

which gives information on heterogeneity of the local dynamics of the system. In equation (2), δ is the delta function. In the calculation of the PDF, the displacements in both x and y directions were used equivalently under the assumption of the isotropy of the systems.

3. Results and discussion

Fig. 1 shows plots of the MSD as a function of the lag time τ obtained at different time t_w after the quench for a gelatin solution of 10 wt%. The double logarithmic plots of the MSD were linear,

$$\langle \Delta r^2(\tau) \rangle \propto \tau^{\alpha}, \qquad (3)$$

in the range of τ for the present study. Here, the exponent α represents the slope of the double logarithmic plots in Fig. 1. In the initial stage from t_w = 10 min to 60 min, the value of α is approximately unity, which follows the relation

$$\langle \Delta r^2(\tau) \rangle = 4D\tau \qquad (4)$$

for the Brownian motion of a particle in a homogeneous Newtonian fluid. In equation (4), D is the diffusion coefficient and is related to the viscosity η of the fluid as $D = kT/(6\pi\eta a)$, where k, T and a are the Boltzmann constant, absolute temperature, and the radius of microspheres, respectively. Fitting of the equation (4) to the MSD at t_w = 20 min gives D = 1.62 × 10^{-14} m^2/s and η = 44.8 mPa s. The plots shifted downward with time retaining the same slope (~ 1) during the initial stage, representing the decrease in D due to the increase in η. In the later stage ($t_w \geq 90$ min), the values of the MSD and α decreased with time and the value of α approached zero. In equation 3, $\alpha = 0$ means that the particles are fluctuating around their equilibrium positions, which indicates that the gelatin behaves as an elastic gel. Thus, the value of α varying from 1 to 0 represents the extent of the sol-to-gel transition. In the region of $0 < \alpha < 1$, the system is viscoelastic and its rheological properties depend on the time scale of observation, τ in the present study. In general, the MSD curves for the viscoelastic media could be locally represented by the equation (3) within a limited range of τ, but the value of α depends on τ (Moschakis, 2013). Only at the sol-gel critical point, the MSD follows equation (3) with a constant α ($0 < \alpha < 1$) in a broad range of τ, where α corresponds to the critical relaxation exponent (Larsen & Furst, 2008; Winter & Chambon, 1986). The linear relation with α of $0 < \alpha < 1$ of the plots in Fig. 1 is at least attributed to the limited range of τ in the present study.

The variation of the MSD due to the gelation occurred in the same manner for gelatin of the other concentrations. The value of α versus t_w for different concentrations (Fig. 2) showed that the gelation rate increased with the gelatin concentration. The dotted lines in Fig. 2 were curves fitted with an empirical equation:

$$\alpha = A \exp[-\Gamma(t_w - t_0)] \qquad (5)$$

defined for $t_w \geq t_0$, where A and Γ are constants and t_0 is the time of onset of viscoelasticity. Using the fitted results, we obtained the gelation time t_{gel} on the basis of a simple definition α = 0.5 (Moschakis, Murray & Dickinson, 2010). The plot of t_{gel} against the gelatin concentration (Fig. 3) indicates the faster gelation process for higher concentrations and moreover, the obtained values of t_{gel} were consistent with those estimated from the data of bulk rheology (Supplementary material, S4).

Fig. 4 shows PDFs for the gelatin solution of 10 wt% measured at t_w = 20 min. In Fig. 4,

179 the PDFs at $x = 0$ were rescaled to be unity, i.e. $P(0, \tau) = 1$. The shape of the PDF broadened
180 with increasing τ, which indicates that the particles can diffuse in the gelatin solution. As
181 shown in Figs. 1 and 2, the gelatin solution behaved as a Newtonian fluid at t_w = 20 min. For
182 a homogeneous Newtonian fluid, $P(x, \tau)$ satisfies the diffusion equation,

183 $$\frac{\partial P}{\partial \tau} = D \frac{\partial^2 P}{\partial x^2}, \qquad (6)$$

184 and is consequently represented by a Gaussian distribution of x as follows,

185 $$P(x, \tau) = \frac{1}{\sqrt{4\pi D\tau}} \exp\left[-\frac{x^2}{4D\tau}\right]. \qquad (7)$$

186 The dotted lines in Fig. 4 show Gaussian distribution functions, which coincide with the
187 observed PDFs. The variances of the Gaussian distributions in Fig. 4 were plotted against τ,
188 showing proportionality between the variance and τ (Fig. 5). According to equation (7), the
189 variance of the Gaussian distribution equals $2D\tau$. The value of $D = 1.65 \times 10^{-14}$ m^2/s obtained
190 from the slope of Fig. 5 almost equals the value of $D = 1.62 \times 10^{-14}$ m^2/s calculated according
191 to equation (4).

192 Fig. 6 shows rescaled PDFs for the gelatin solution of 10 wt% measured at t_w = 360 min.
193 The dotted lines in Fig. 6 again show Gaussian distribution functions. Figs. 1 and 2 indicate
194 that the gelatin can be regarded as an elastic solid at t_w = 360 min. As shown in Fig. 6, the
195 shape of the PDF did not vary with τ. This is attributable to the hindrance to the diffusion of
196 the particles, indicating the elastic nature of the gelatin. Moreover, the shape of the observed
197 PDF obviously deviated from that of the Gaussian distribution function. This result is due to
198 heterogeneous local dynamics of the gelatin gel, as discussed in detail later.

199 The variation of the PDF at τ = 1.25 s for the gelatin solution of 10 wt% was shown in Fig.
200 7. The shape of the PDF narrowed with t_w, which indicates the decrease in mobility of the
201 particles with time due to the gelation. The PDFs were Gaussian for short times after the
202 quench, but became non-Gaussian showing broad tails for longer times.

203 The non-Gaussian PDF with a long exponential tail has been associated with
204 spatio-temporal heterogeneity of dynamics, and is obtained from various theoretical models
205 such as the random walk with a special probability density function for waiting-time and a
206 jump-length (continuous-time random walk, CTRW) (Metzler & Klafter, 2000), the diffusion

on fractal geometries (Havlin & Ben-Avraham, 1987), and the diffusion with fluctuating diffusivity (Chechkin, Seno, Metzler & Sokolov, 2017). The deviation from the Gaussian distribution and the appearance of a broad tail in the PDF has been recognized as a signature of glassy dynamics (Chaudhuri, Berthier & Kob, 2007). This is attributed to dynamic heterogeneity caused by two families of particles constituting glassy systems: particles that perform localized, vibrational motion in "cages" of their neighbors and particles that perform quasi-instantaneous jump escaping from the "cages" (Chaudhuri et al., 2007). Previous studies showed that gelatin exhibited the continuous restructuring of the network for a long time period (aging) after the percolated network formation (Normand et al., 2000; Ronsin et al., 2009; Te Nijenhuis, 1981a) and various hysteretic behaviors (Parker & Normand, 2010; Ronsin et al., 2009; Te Nijenhuis, 1981b), which were reminiscent of glassy systems. Thus, it is intriguing that the PDF of the probe particles embedded in gelatin gels (Fig. 6) is similar to that in the glassy systems. In order to evaluate this apparent similarity, we investigated the origin of the non-Gaussianity of the PDF for the gelatin gels as shown below.

For the further analysis of the PDF in the gel state (Fig. 6), we calculated the PDF of the displacement for each particle, defined as

$$P_i(x,\tau) = \langle \delta(x - [x_i(t+\tau) - x_i(t)]) \rangle, \qquad (8)$$

although the information extracted from individual trajectories is somewhat limited in statistics. Some typical PDFs for each particle were shown in Fig. 8. The PDFs are substantially different in the width from each other, but all of them follow Gaussian distribution functions (dotted lines). Thus, the non-Gaussian PDF as shown in Fig. 6 originated from the superposition of a number of Gaussian PDFs with different widths as shown in Fig. 8. Because the shape of the PDF in the gel state did not vary with τ, the mechanism for the Gaussian PDFs in Fig. 8 should not be due to the free diffusion of the particles as described by equation (7). In the case that a particle is surrounded by an elastic gel, the displacement of the particle will fluctuate around its equilibrium position. If this situation is regarded as the case that the particle is trapped in a potential $U(x)$, $P_i(x, \tau)$ follows a Boltzmann distribution as follows,

$$P_i(x,\tau) = P_0 \exp\left[-\frac{U(x)}{kT}\right], \qquad (9)$$

where P_0 is a constant. When $U(x)$ can be approximated as a harmonic potential with a spring constant κ, i.e. $U(x) = \frac{1}{2}\kappa x^2$, equation (9) is written as Gaussian distribution,

$$P_i(x,\tau) = P_0 \exp\left[-\frac{x^2}{\sigma^2}\right], \qquad (10)$$

where $\sigma^2 = 2kT/\kappa$. Since κ reflects the rigidity of the surrounding gel, the different widths of the PDFs for each particle (Fig. 8) are attributable to spatial inhomogeneity in the gel rigidity. We note that this inhomogeneity is an intrinsic property of the gelatin gel and not due to the reason such as the local gradient of temperature because the rigidity distribution was random in the field of view (Supporting material, S5).

The origin of the non-Gaussian PDF of gelatin (Fig. 6) is different from that of either glassy systems or gelling systems measured by multiple particle tracking in previous studies. In glassy systems, a particle localized in a cage can occasionally jump from the cage and therefore the coexistence of the slow and fast particles is dynamically generated (Chaudhuri et al., 2007), resulting in the non-Gaussian PDF for each particle. The non-Gaussianity due to the same mechanism was reported in the study of the tracking of diffusing quantum dots in heterogeneous polyacrylamide gels (Lee, Crosby, Emrick & Hayward, 2013). This type of dynamics can be described by the CTRW model (Chaudhuri et al., 2007; Lee et al., 2013) and in this case the MSD shows a subdiffusive behavior (Metzler & Klafter, 2000, Lee et al., 2013). For the gelatin in the gel state, in contrast, the PDF for each particle was Gaussian and the MSD showed a solid-like behavior. The non-Gaussian PDF observed in the gelation of barley β-glucan was associated with the separated groups of freely diffusing particles and trapped particles as seen from the MSD for each particle (Moschakis, Lazaridou & Biliaderis, 2012). On the other hand, such separation was not observed in the MSD for each particle in the present study (data not shown) and therefore we can conclude that the non-Gaussian PDF in the gelatin gel was due to the spatial variation of the gel rigidity.

The coefficient of variation (CV) of σ, i.e. the standard deviation of σ divided by the mean value of σ, is a useful quantity for estimating the rheological inhomogeneity of the gelatin, since σ in equation (10) is related to the local dynamics of gelatin. The CV of σ at τ = 1.25 s for the gelatin solution of 10 wt% was presented as a function of t_w in Fig. 9, together with the exponent α of MSD. The CV was almost constant until t_w = 100 min, and then increased

steeply. The increase in the CV coincided with the decrease in α. Fig. 10 shows the correlation between the CV and α for the gelatin solutions with different concentrations. The data of different concentrations are scattering around a single curve and the CV increased with the decrease in α for any concentrations. Thus, it is concluded that the rheological inhomogeneity developed in parallel with the elastic behavior of gelatin.

In a previous study, Hong et al. carried out the multiple particle tracking experiments on the gelatin obtained from porcine skin and observed the non-Gaussian PDF during the time-dependent sol-gel transition (Hong et al., 2018). They focused on the particle diffusivity derived from the PDF of the short τ region (τ = 0.033 s), and found that the non-Gaussianity spiked twice in the pre-gel stage and then increased again in the post-gel stage. They attributed the non-Gaussian PDF in the pre-gel stage to the bifurcation of diffusivity of the particles and that in the post-gel stage to the inhomogeneity of the gel network, although the latter was not discussed in detail. In contrast to the previous study, the PDFs observed in the pre-gel stage were all Gaussian in the present study. The reason for this inconsistency is unclear, but may be due to limited statistics in the previous study owing to the fast gelation of porcine gelatin. On the other hand, the non-Gaussian PDF stemming from the rheological inhomogeneity was observed in the post-gel region in the present study, which would be equivalent to that was reported previously as the third appearance of the non-Gaussianity.

The fish gelatin used in the present study was extracted from the skin of two different fish species. It has been reported for blends of different gelatins that helix renaturation occurred mainly through the association of the chains from the same species (Joly-Duhamel, Hellio & Djabourov, 2002). This implies that mixed gelatins from different species would form more heterogeneous gels at the molecular level compared to gelatins from a single source. The effect of the composition of the gelatin is, however, not the main reason for the rheological inhomogeneity observed in this study because the non-Gaussian PDF in the gel state was observed also for the porcine skin gelatin (Supplementary material, S6). The rheological inhomogeneity in the micron scale for the gelatin gels demonstrated in the present study is likely due to the frozen density fluctuation which causes the speckle pattern of the scattered light (Okamoto et al., 2001), as both the rheological inhomogeneity and the speckle pattern appeared immediately after the gel formation. We note that the non-Gaussian PDF for the

porcine gelatin appeared relatively soon after the quench despite the lower concentration (within 30 min for 5 wt% gelatin) (Supplementary material, S6). This represents the slower gelation of fish gelatins compared to mammalian gelatins, which is associated with the smaller quench depth due to the lower gelation temperature for fish gelatins. The quantitative comparison of the gelation behaviors between fish and mammalian gelatins by the multi-particle tracking method is a scope of our ongoing work.

In conclusion, the gelation process of fish gelatin was investigated by the multiple particle tracking method in detail, taking advantage of the slow gelation of the fish gelatin. As the gelation proceeded, the exponent α of the MSD varied from 1 to 0, indicating the transition from fluid-like behaviors to solid-like behaviors. In the fluid state ($\alpha \sim 1$), the shape of the PDF for the particle displacement was Gaussian and broadened with the lag time τ, which shows that the gelatin solution was regarded as a homogeneous Newtonian fluid. In the elastic gel state ($\alpha \sim 1$), on the other hand, the shape of the PDF was non-Gaussian and was independent of τ. The non-Gaussianity was attributed to the inhomogeneity of the rigidity of the gelatin gel at the micron scale, since the PDFs for each particle were represented by the Gaussian distribution function with different widths. Therefore, although the shape of the non-Gaussian PDF of the gelatin gel was reminiscent of that of glassy systems, the mechanisms for the non-Gaussianity were different from each other. The growth of the inhomogeneity of the local dynamics was correlated with the development of elastic properties induced by the gelation.

Acknowledgement

This work was supported by JSPS KAKENHI (Grants-in-Aid for Scientific Research) Grant Number 15K20906 and 18K05519.

References

Bode, F., da Silva, M. A., Smith, P., Lorenz, C. D., McCullen, S., Stevens, M. M., & Dreiss, C. A. (2013). Hybrid gelation processes in enzymatically gelled gelatin: Impact on nanostructure, macroscopic properties and cellular response. *Soft Matter*, *9*, 6986-6999.

Breedveld, V., & Pine, D. J. (2003). Microrheology as a tool for high-throughput screening. *Journal of Materials Science*, *38*, 4461-4470.

Chaudhuri, P., Berthier, L., & Kob, W. (2007). Universal nature of particle displacement close to glass and jamming transitions. *Physical Review Letters*, *99*, 060604.

Chechkin, A. V., Seno, F., Metzler, R., & Sokolov, I. M. (2017). Brownian yet non-Gaussian diffusion: From superstatistics to subordination of diffusing diffusivities. *Physical Review X*, *7*, 021002.

Djabourov, M., Leblond, J., & Papon, P. (1988). Gelation of aqueous gelatin solutions. I. Structrural investigation., *Journal de Physique France*, *49*, 319-332.

Furst, E. M., & Squires, T. M. (2017). *Microrheology*, Oxford University Press.

Havlin, S., & Ben-Avraham, D. (1987). Diffusion in disordered media. *Advances in Physics*, *36*, 695-798.

Hong, W., Xu, G., Ou, X., Sun, W., Wang, T., & Tong, Z. (2018). Colloidal probe dynamics in gelatin solution during the sol-gel transition. *Soft Matter*, *14*, 3694-3703.

Joly-Duhamel, C., Hellio, D., & Djabourov, M. (2002). All gelatin networks: 1. Biodiversity and physical chemistry. *Langmuir*, *18*, 7208-7217.

Karim, A. A., & Bhat R. (2009). Fish gelatin: properties, challenges, and prospects as an alternative to mammalian gelatins. *Food Hydrocolloids*, *23*, 563-576.

Larsen, T. H., & Furst, E. M. (2008). Microrheology of the liquid-solid transition during gelation. *Physical Review Letters*, *100*, 146001.

Lee, C. H., Crosby, A. J., Emrick, T., & Hayward, R. C. (2014). Characterization of heterogeneous polyacrylamide hydrogels by tracking of single quantum dots. *Macromolecules*, *47*, 741-749.

Lin, L., Regenstein, J. M., Lv, S., Lu, J., & Jiang, S. (2017). An overview of gelatin derived from aquatic animals: Properties and modification. *Trends in Food Science & Technology*, *68*, 102-112.

Lu, J., & Corvalan, C. M. (2016). Soft food microrheology. *Current Opinion in Food Science*, *9*, 112-116.

Metzler, R., & Klafter, J. (2000). The random walk's guide to anomalous diffusion: a fractional dynamics approach. *Physics Reports*, *339*, 1-77.

354 Morita, T., Narita, T., Mukai, S., Yanagisawa, M., & Tokita, M. (2013). Phase behaviors of
355 agarose gel. *AIP Advances*, *3*, 042128.
356 Moschakis, T. (2013). Microrheology and particle tracking in food gels and emulsions.
357 *Current Opinion in Colloid & Interface Science*, *18*, 311-323.
358 Moschakis, T., Lazaridou, A., & Biliaderis, C. G. (2012). Using particle tracking to probe the
359 local dynamics of barley β-glucan solutions upon gelation. *Journal of Colloid and*
360 *Interface Science*, *375*, 50-59.
361 Moschakis, T., Murray, B. S., & Dickinson, E. (2010). On the kinetics of acid sodium
362 caseinate elation using particle tracking to probe the microrheology. *Journal of Colloid*
363 *and Interface Science*, *345*, 278-285.
364 Normand, V., Muller, S., Ravey, J-C., & Parker, A. (2000). Gelation kinetics of gelatin: A
365 master curve and network modeling. *Macromolecules*, *33*, 1063-1071.
366 Okamoto, M., Norisuye, T., & Shibayama, M. (2001). Time-resolved dynamic light scattering
367 study on gelation and gel-melting processes of gelatin gels. *Macromolecules*, *34*,
368 8496-8502.
369 Parker, A., & Normand, V. (2010). Glassy dynamics of gelatin gels. *Soft Matter*, *6*,
370 4916-4919.
371 Pezron, I., Herning, T., Djabourov, M., & Leblond, J. (1990). Scattering from a biopolymer
372 solution in sol and gel states: The gelatin example. In S. B. Ross-Murphy & W. Burchard
373 (Eds.), *Physical Networks*, Elsevier Applied Science.
374 Ronsin, O., Caroli, C., & Baumberger, T. (2009). Interplay between shear loading and
375 structural aging in a physical gelatin gel. *Physical Review Letters*, *103*, 138302.
376 Ronsin, O., Caroli, C., & Baumberger, T. (2017). Preferential hydration fully controls the
377 renaturation dynamics of collagen in water-glycerol solvents, *European Physical Journal*
378 *E*, *40*, 55.
379 Ross-Murphy, S. B. (1992). Structure and rheology of gelatin gels: Recent progress. *Polymer*,
380 *33*, 2622-2627.
381 Savin, T., & Doyle, P. S. (2005). Static and dynamic errors in particle tracking microrheology.
382 *Biophysical Journal*, *88*, 623-638.

Shabaniverki, S., & Juárez, J. J. (2017). Characterizing gelatin hydrogel viscoelasticity with diffusing colloidal probe microscopy. *Journal of Colloid and Interface Science*, *497*, 73-82.

Shibayama, M. (1998). Spatial inhomogeneity and dynamic fluctuations of polymer gels. *Macromolecular Chemistry and Physics*, *199*, 1-30.

Te Nijenhuis, K. (1981a). Investigation into the ageing process in gels of gelatin/water systems by the measurement of their dynamic moduli. Part I: Phenomenology. *Colloid and Polymer Science*, *259*, 522-535.

Te Nijenhuis, K. (1981b). Investigation into the ageing process in gels of gelatin/water systems by the measurement of their dynamic moduli. Part II: Mechanism of the ageing process. *Colloid and Polymer Science*, *259*, 1017-1026.

Weel, K. G. C., Boelrijk, A. E. M., Alting, A. C., van Mil, P. J. J. M., Burger, J. J., Gruppen, H., Voragen, A. G. J., & Smit, G. (2002). Flavor release and perception of flavored whey protein gels: Perception is determined by texture rather than by release. *Journal of Agricultural and Food Chemistry*, *50*, 5149-5155.

Winter, H. H., & Chambon, F. (1986). Analysis of linear viscoelasticity of a crosslinking polymer at the gel point. *Journal of Rheology*, *30*, 367-382.

Yang, K., Wang, Z., Brenner, T., Kikuzaki, H., Fang, Y., & Nishinari, K. (2015). Sucrose release from agar gels: Effects of dissolution order and the network inhomogeneity. *Food Hydrocolloids*, *43*, 100-106.

Yang, Z., Hemar, Y., Hilliou, L., Gilbert, E. P., McGillivray, D. J., Williams, M. A. K., & Chaieb, S. (2016). Nonlinear behavior of gelatin networks reveals a hierarchical structure. *Biomacromolecules*, *17*, 590-600.

Yoshimura, K., Terashima, M., Hozan, D., Ebato, T., Nomura, Y., Ishii, Y., & Shirai, K. (2000). Physical properties of shark gelatin compared with pig gelatin. *Journal of Agricultural and Food Chemistry*, *48*, 2023-2027.

Figure captions

Fig. 1. MSD as a function of the lag time τ measured at t_w = 10, 20, 30, 60, 90, 120, 180, 240, 300, 360 min (from top to bottom) for a gelatin solution of 10 wt%. The dashed and dashed-dotted lines represent straight lines with a slope of 1 and 0, respectively.

Fig. 2. Exponent α of MSD versus t_w for the gelatin concentration of 7.5 wt% (●), 10 wt% (●), 12.5 wt% (●) and 15 wt% (●). The dotted lines were curves fitted with equation (5).

Fig. 3. Dependence of the gelation time t_{gel} on the gelatin concentration.

Fig. 4. PDF of τ = 1.25 s (●), 3.13 s (●), and 5.00 s (●) measured at t_w = 20 min for 10 wt% gelatin. The dotted lines represent Gaussian distribution functions.

Fig. 5. The variances of the Gaussian distributions shown in Fig. 4 plotted against τ.

Fig. 6. PDF of τ = 1.25 s (●), 3.13 s (●), and 5.00 s (●) measured at t_w = 360 min for 10 wt% gelatin. The dotted lines represent Gaussian distribution functions.

Fig. 7. (a) PDF of τ = 1.25 s measured at t_w = 30 min (●), 90 min (●), 180 min (●), and 360 min (●) for 10 wt% gelatin. The dotted lines represent Gaussian distribution functions. (b) The small x region of (a) was expanded.

Fig. 8. Typical PDFs of the displacement for each particle (τ = 1.25 s) measured at t_w = 360 min for 10 wt% gelatin. The dotted lines represent Gaussian distribution functions.

Fig. 9. CV of σ at τ = 1.25 s and the value of α versus t_w for 10 wt% gelatin.

Fig. 10. Correlation between the CV of σ at τ = 1.25 s and the value of α for the gelatin at the concentration of 7.5 wt% (●), 10 wt% (■), 12.5 wt% (▲), and 15 wt% (◆).

Fig. 1

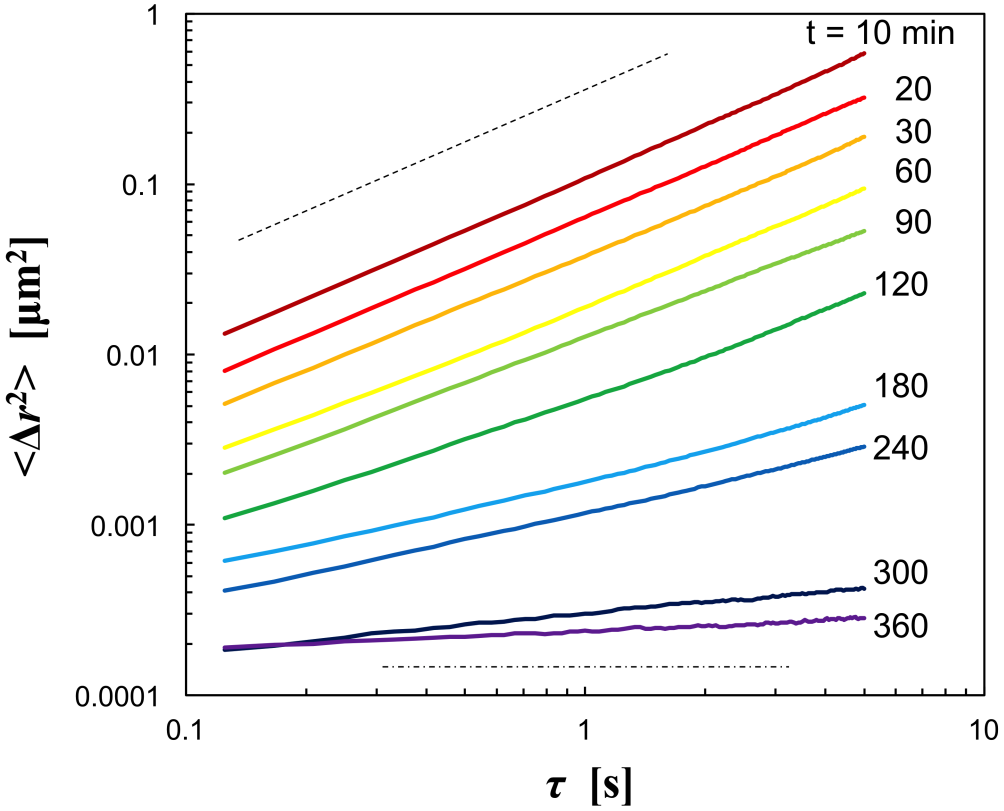

Fig. 2

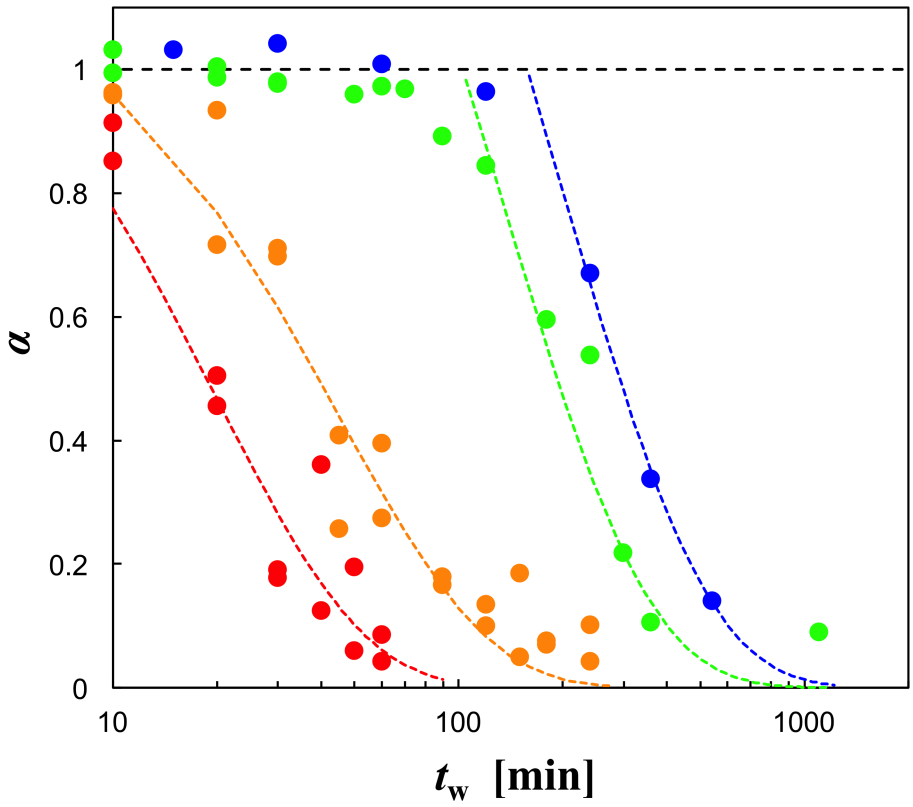

Fig. 3

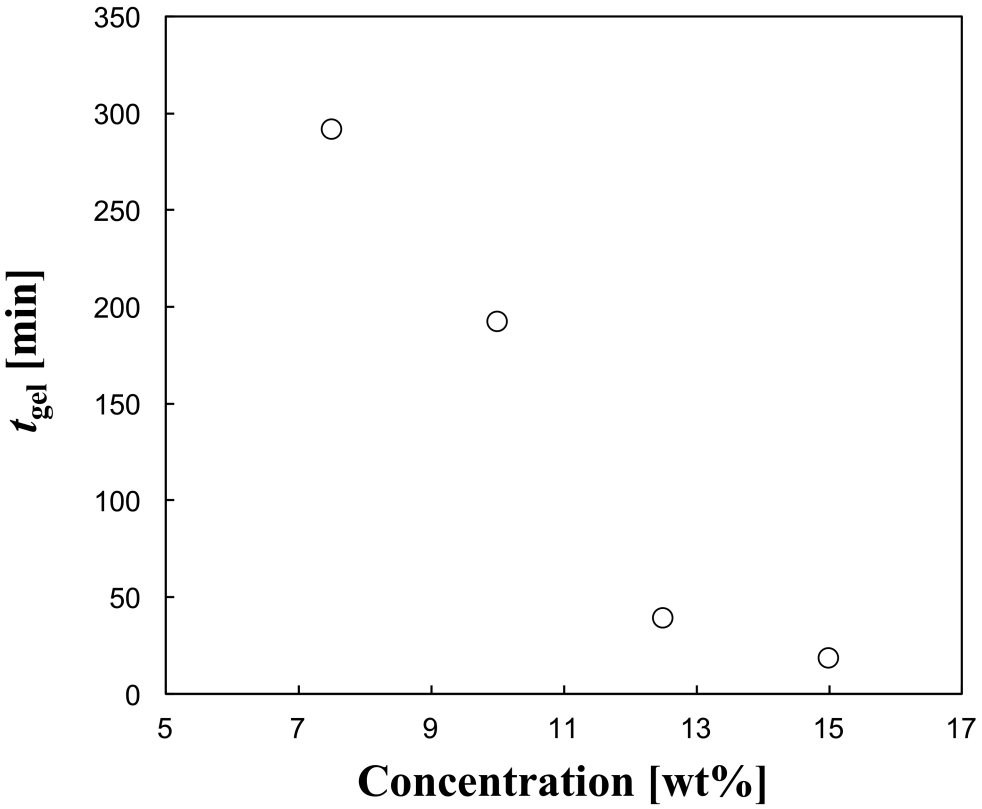
350
300
250
200
150
100
50
0
5
7
9
11
13
15
17
t_{gel} [min]
Concentration [wt%]

Fig. 4

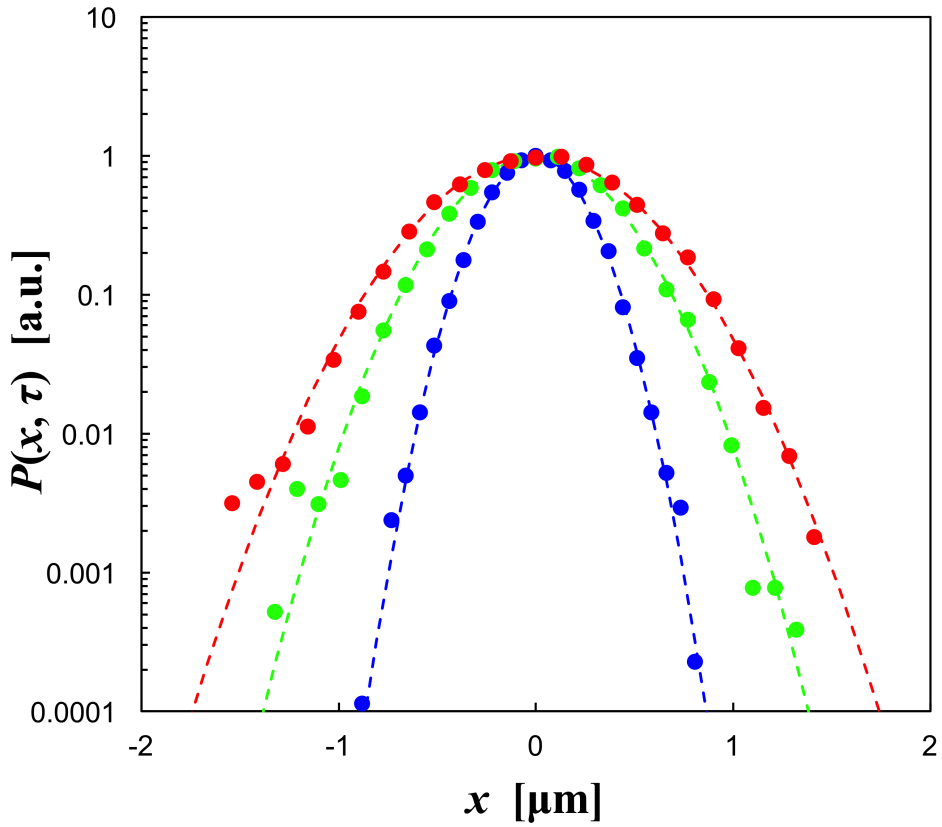

Fig. 5

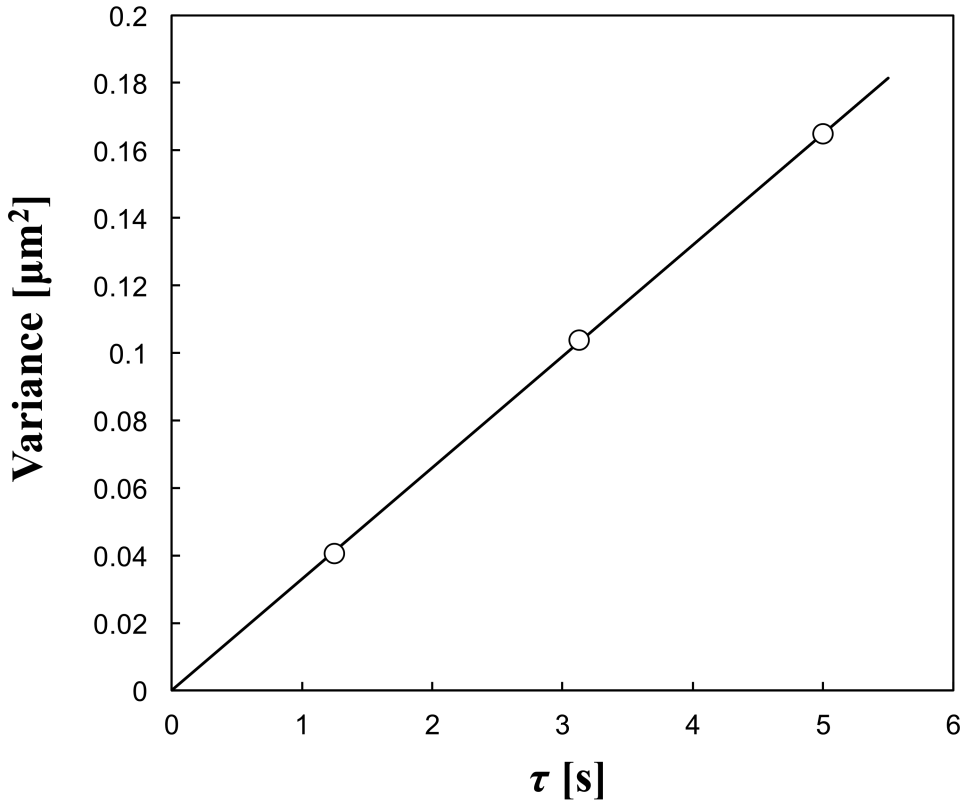

Fig. 6

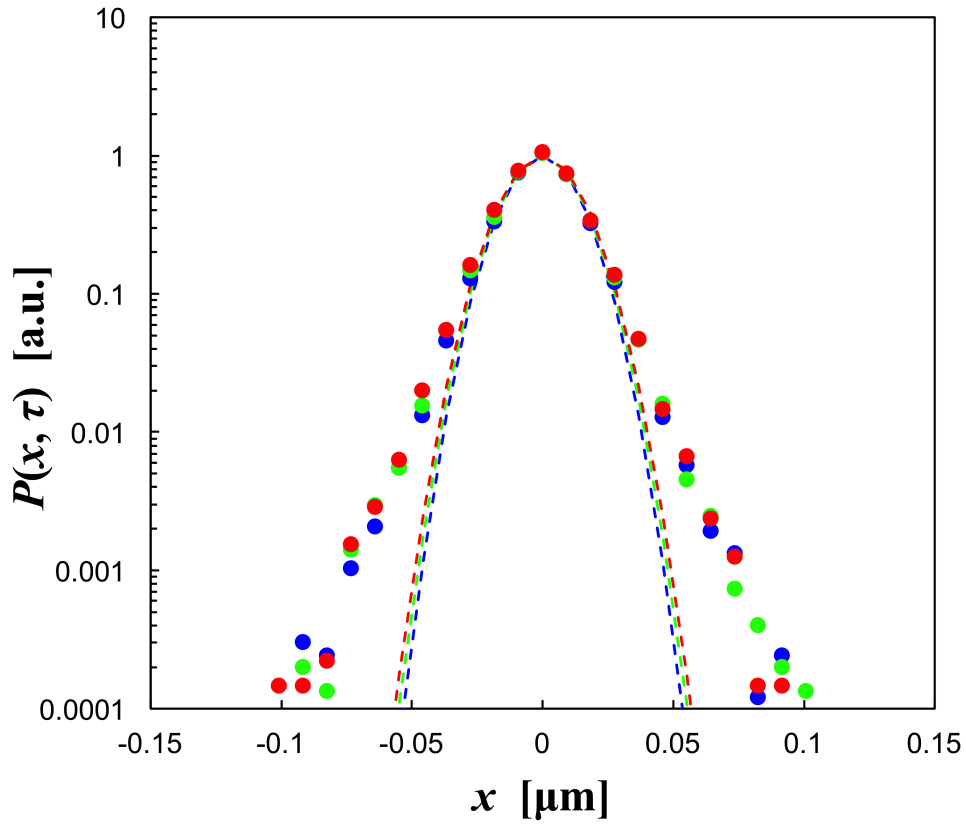

557

558

559

560 Fig. 7

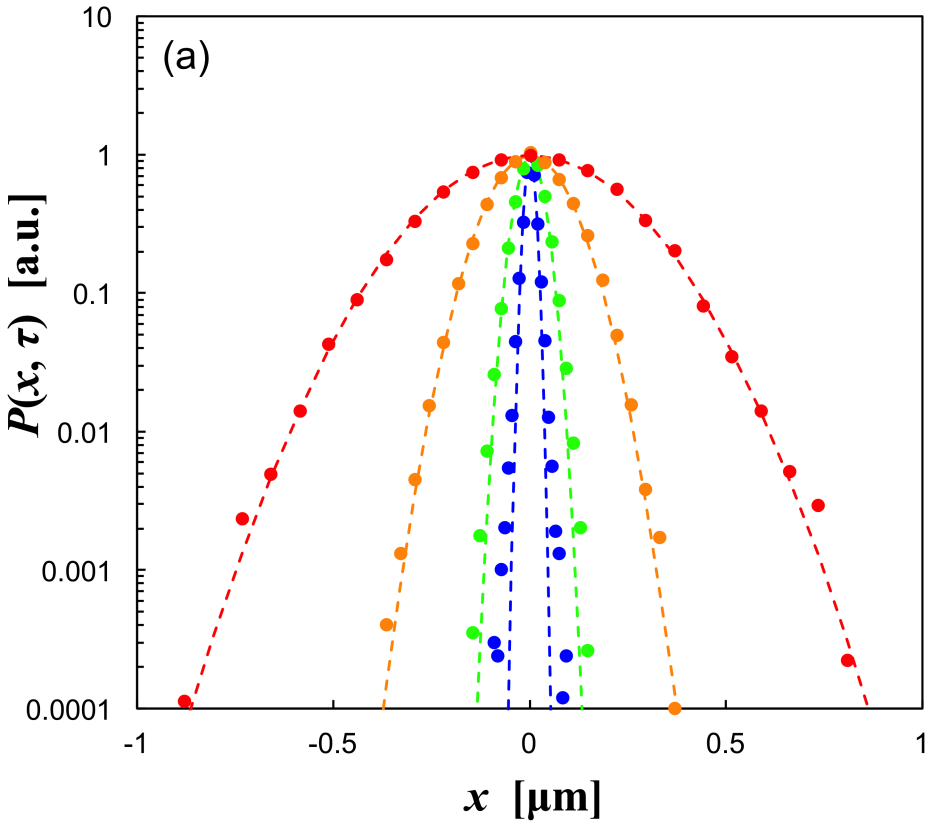

561

562

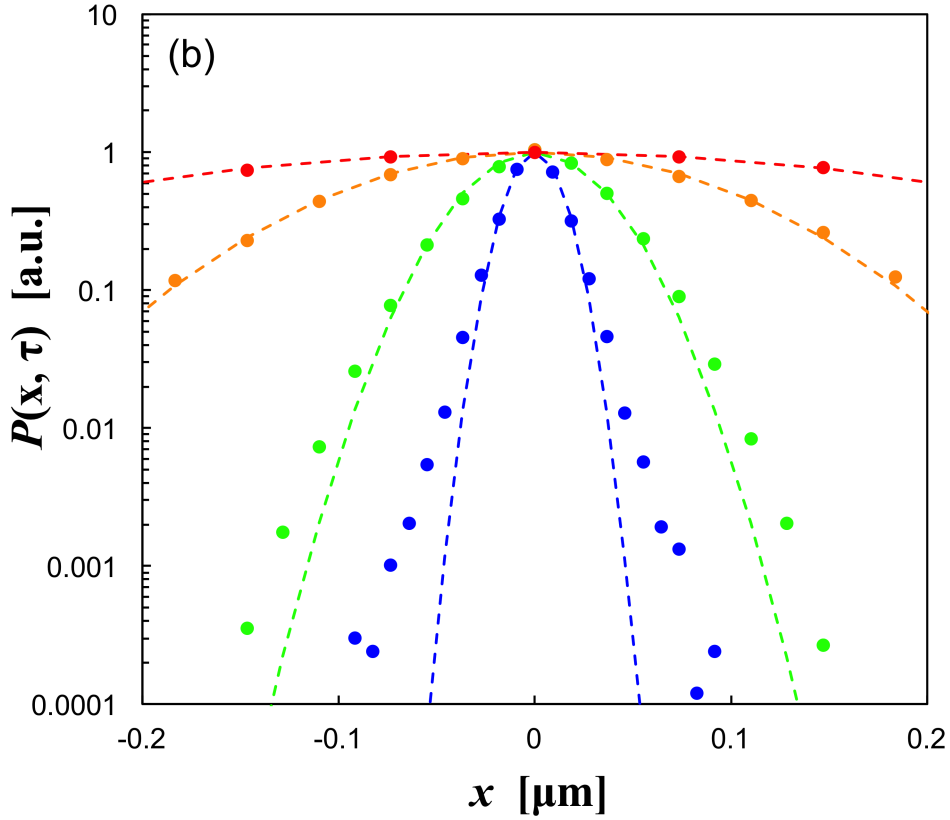

563

564 Fig. 8

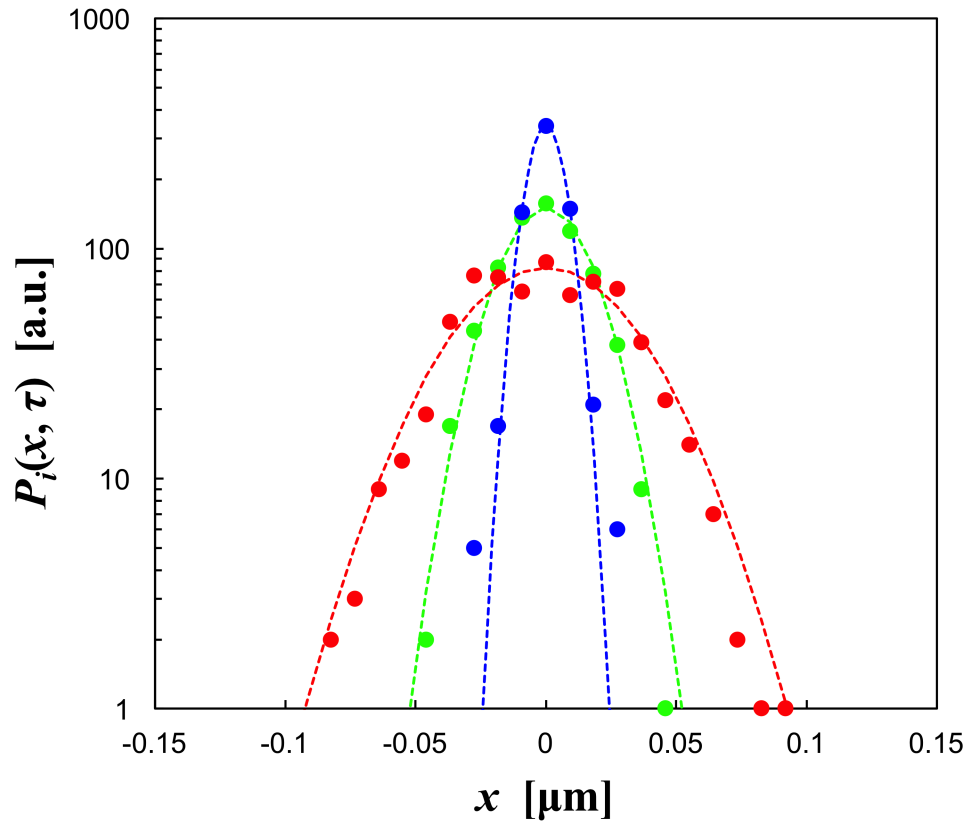

565

566

Fig. 9

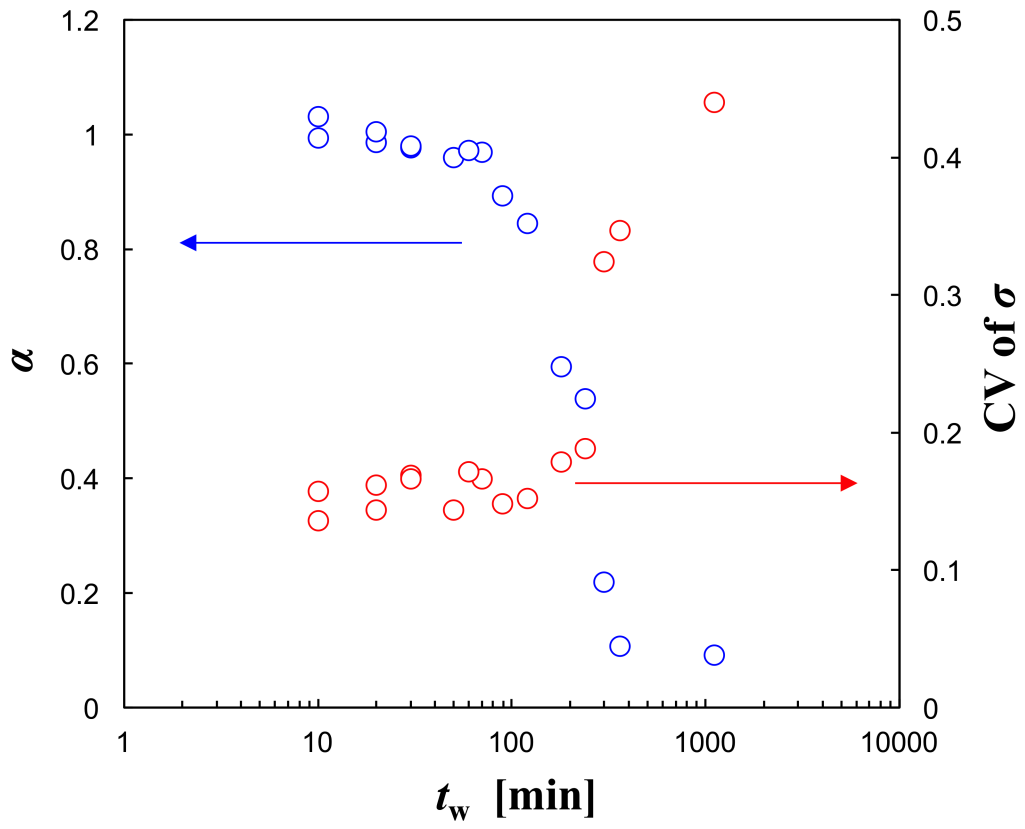

584
585
586
587
588
589
590
591
592
593
594
595
596
597
598 Fig. 10

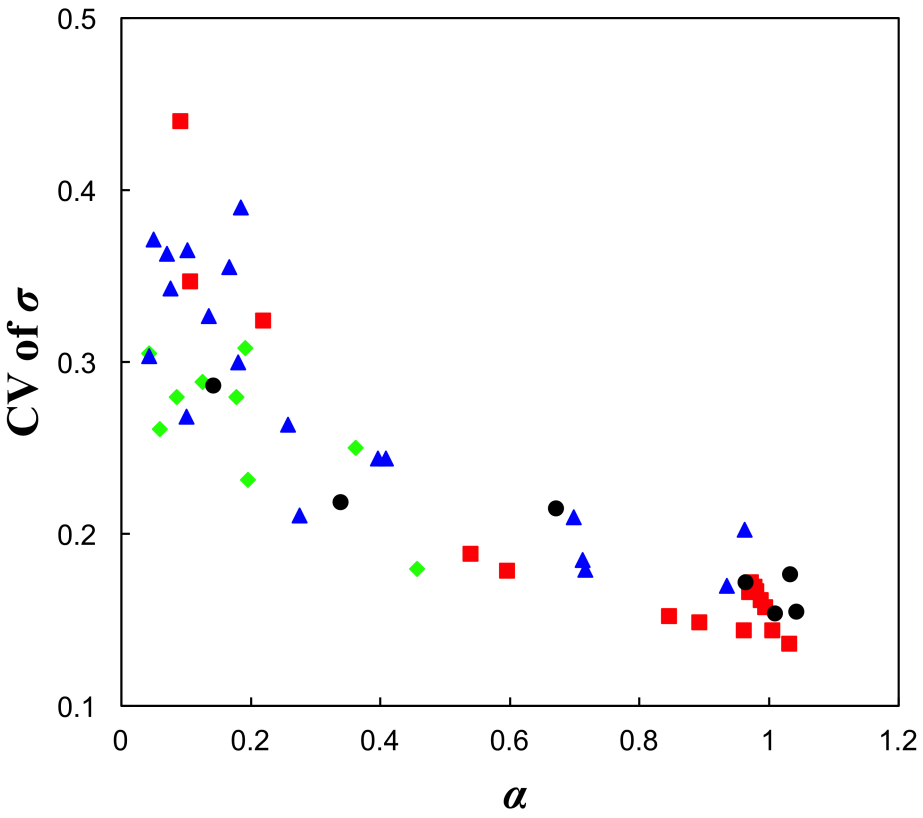

599
600

601

602

603

604

605

606

607

608

609

610